Biochimica et Biophysica Acta 1852 (2015) 2066–2074

Contents lists available at ScienceDirect

Biochimica et Biophysica Acta

journal homepage: www.elsevier.com/locate/bbadis

# Impaired enzymatic defensive activity, mitochondrial dysfunction and proteasome activation are involved in RTT cell oxidative damage

Carlo Cervellati [a,1], Claudia Sticozzi [b,1], Arianna Romani [a], Giuseppe Belmonte [b], Domenico De Rasmo [c], Anna Signorile [d], Franco Cervellati [b], Chiara Milanese [e], Pier Giorgio Mastroberardino [e], Alessandra Pecorelli [f], Vinno Savelli [g], Henry J. Forman [h,i], Joussef Hayek [f,2], Giuseppe Valacchi [b,j,*,2]

[a] Department of Biomedical and Specialist Surgical Sciences, Section of Medical Biochemistry, Molecular Biology and Genetics, University of Ferrara, Ferrara, Italy
[b] Department of Life Sciences and Biotechnology, University of Ferrara, 44121 Ferrara, Italy
[c] Institute of Biomembrane and Bioenergetics, CNR, Bari 70124, Italy
[d] Department of Basic Medical Sciences, Neurosciences and Sense Organs, University of Bari "Aldo Moro", Bari 70124, Italy
[e] Department of Genetics, Erasmus University Medical Center Rotterdam, the Netherlands
[f] Child Neuropsychiatry Unit, University Hospital, Azienda Ospedaliera Universitaria Senese (AOUS), Siena, Italy
[g] Dipartimento di Scienze Mediche, Chirurgiche e Neuroscienze, Universita' di Siena, 53100 Siena, Italy
[h] Davis School of Gerontology, University of Southern California, Los Angeles, CA 90089, USA
[i] Life and Environmental Sciences Unit, University of California at Merced, Merced, CA 95344, USA
[j] Department of Food and Nutrition, Kyung Hee University, 1 Hoegi-dong, Dongdaemun-gu, Seoul 130-701, Republic of Korea

ARTICLE INFO

*Article history:*
Received 11 May 2015
Received in revised form 7 July 2015
Accepted 15 July 2015
Available online 17 July 2015

*Keywords:*
Oxidative stress
NADPH oxidase
Glutathione peroxidase
Superoxide dismutase thioredoxin-reductases
4HNE

ABSTRACT

A strong correlation between oxidative stress (OS) and Rett syndrome (RTT), a rare neurodevelopmental disorder affecting females in the 95% of the cases, has been well documented although the source of OS and the effect of a redox imbalance in this pathology has not been yet investigated. Using freshly isolated skin fibroblasts from RTT patients and healthy subjects, we have demonstrated in RTT cells high levels of $H_2O_2$ and HNE protein adducts. These findings correlated with the constitutive activation of NADPH-oxidase (NOX) and that was prevented by a NOX inhibitor and iron chelator pre-treatment, showing its direct involvement. In parallel, we demonstrated an increase in mitochondrial oxidant production, altered mitochondrial biogenesis and impaired proteasome activity in RTT samples. Further, we found that the key cellular defensive enzymes: glutathione peroxidase, superoxide dismutase and thioredoxin reductases activities were also significantly lower in RTT. Taken all together, our findings suggest that the systemic OS levels in RTT can be a consequence of both: increased endogenous oxidants as well as altered mitochondrial biogenesis with a decreased activity of defensive enzymes that leads to posttranslational oxidant protein modification and a proteasome activity impairment.


## 1. Introduction

Rett syndrome (RTT) (OMIM ID: 312750) is a severe neurological disorder that affects almost exclusively females, with a frequency of approximately 1:10,000 live births. Patients affected by RTT typically exhibit various neuropsychiatric features after 6–18 months [1] of apparently normal neurodevelopment. Afterwards, they fall into developmental stagnation followed by rapid and sharp deterioration, featuring loss of previously acquired speech, replacement of purposeful use of the hands with incessant stereotypies, which are characteristic of the syndrome. Mutations in the X-linked gene encoding the Methyl-CpG-binding protein 2 (MECP2) account for approximately 90% of cases with typical RTT and are almost exclusively de novo. MeCP2, a key transcriptional regulator, is critically involved in gene silencing through methylation-dependent remodeling of chromatin structure.

Despite almost two decades of research into the functions and role of MeCP2, surprisingly little is known about the mechanisms leading from MeCP2 deficiency to disease expression, with many questions left regarding the role of MeCP2 in brain and, more in general, during development and in physiopathology [2]. Restoration of Mecp2 function in astrocytes alone significantly improves the developmental outcome of Mecp2-null mice [3], thus suggesting that RTT can be reversible upon restoration of the Mecp2 function [4].

In the last few years, we have demonstrated a condition of systemic oxidative stress in human patients with typical RTT as indicated by increased levels of F2- and F3-isoprostanes (IsoPs) and F4-neuroprostanes (NeuroPs), NPBI (Non Protein Bound Iron), and 4-hydroxy-2-nonenal (HNE) protein adducts in the plasma of RTT patients. In particular, high

* Corresponding author at: Dept. Life Sciences (Life Sciences) and Biotechnology (Biotechnology), University of Ferrara, Via Borsari, 46, 44100 Ferrara, Italy.
*E-mail address:* giuseppe.valacchi@unife.it (G. Valacchi).
[1] Co-first author.
[2] Equally supervised the work.

http://dx.doi.org/10.1016/j.bbadis.2015.07.014
0925-4439/

levels of IsoPs and HNE, which are major lipid peroxidation products generated from membrane lipids by free radical reactions, are strongly associated with the disease natural history, genotype-phenotype correlation, clinical heterogeneity and severity of the disease [5–8].

Likewise, our recent work in RTT murine models suggests that the presence of systemic oxidative stress (OS) precedes the onset of clinical symptoms in RTT mouse model and can be rescued by MeCP2 gene re-expression in the brain of the null mice [9]. Therefore, clinical and experimental evidence supports the concept that oxidative damage plays a previously unrecognized key role in the pathogenesis of RTT/MeCP2 deficiency.

Regardless, the molecular pathways linking the MeCP2 gene mutation to the OS derangement remain to be explored and, in particular, whether the nature of the increase OS present in RTT patients derives from a corrupted defensive enzyme activation or an increased endogenous production of oxidants, or both, needs still to be investigated.

In the present study, we attempt to investigate the possible mechanistic pathways leading to the altered redox state associated to RTT. Thanks to the use of primary fibroblasts isolated from patients skin biopsies, we investigated the activation of a series of enzymes involved with either the generation of $O_2^{\cdot-}$ or $H_2O_2$ (NADPH oxidase, NOX) or involved in cellular redox defense superoxide dismutase (SOD), glutathione peroxidase (GPx) and catalase (CAT). In addition, as mitochondria are a major cellular source of OS, we have analyzed its functional state as well as the activity of the proteasome machinery. Our data showed that RTT cells have an impaired defensive enzyme activity, increased endogenous oxidant production, altered bioenergetic parameters, and compromised proteasome activity.

## 2. Methods

### 2.1. Study approval

A total of 15 female patients with classical RTT syndrome (mean age: 20.3 ± 12.3), and 15 healthy female controls of comparable age (mean age: 19.2 ± 14.5) participated to the study. All the patients were consecutively admitted to the Child Neuropsychiatry Unit of the University Hospital of Siena (Head: J.H.). Control skin biopsies were carried out during routine health, or donations, while skin biopsies from RTT patients were obtained during the periodic clinical checks-up. The study was approved by the Institutional Review Board of University Hospital, Azienda Ospedaliera Universitaria Senese (AOUS), Siena, Italy and all informed consents were obtained in written form from either the parents or the legal tutors of the enrolled patients. This procedure is approved by the Institutional Review Board of University Hospital, Azienda Ospedaliera Universitaria Senese (15/09/2014).

### 2.2. Human skin fibroblast cultures

Human skin fibroblasts were isolated from 3-mm skin punch biopsy ($n = 6$ for RTT and $n = 6$ for controls) as previously described [32]. Fibroblasts were marked with Vimentin for authentication of cells and tested for mycoplasma contamination (data not shown), before the experimental procedure.

Fibroblasts from passage 3 to 5 were used for the experiments. For experiments with diphenyleneiodonium chloride (DPI, a general inhibitor of flavoproteins including NOX) (Calbiochem, Mialno, Italy) or Desferal (Iron chelator) (Sigma Aldrich, Milan, Italy) the cells were either treated with or without DPI or Desferal (final concentration in culture 10 and 400 μM, respectively) dissolved in DMSO (final concentration in culture 0.01%), and incubated for 2 or 1 h at 37 °C, respectively.

### 2.3. Immunocytochemistry

Fibroblasts were grown on coverslips at a density of $5 \times 10^4$ cell/ml, and then fixed in 4% paraformaldehyde in PBS for 30 min at 4 °C as previously described [10]. After permeabilization the coverslips were blocked in PBS (1% BSA) at room temperature for 1 h. Coverslips were then incubated with primary and then with secondary antibodies. Nuclei were stained with 1 μg/ml DAPI (Molecular Probes) after removal of secondary antibodies. Coverslips were examined by the Leica light microscope equipped with epifluorescence at 63× magnification. Negative controls for the immunostaining experiments were performed by omitting primary antibodies. Images were acquired and analyzed with LEICA CTR6500 HS-Integrated System Solution for Live Cell Imaging and Analysis (Leica Microsystems—Germany).

### 2.4. HNE protein adducts determination

HNE protein adducts were measured by using an enzyme immunoassay OxiSelect HNE-His adduct kit (Cell biolabs, Inc.). The quantity of HNE adduct in protein samples was determined by comparing its absorbance with that of a known HNE-BSA standard curve, according to the manufacturer's instructions.

### 2.5. Assays for oxidants

$H_2O_2$ coming from cells into the medium was measured using Amplex Red Hydrogen Peroxide/Peroxidase assay kit (Life Technologies). The quantity of $H_2O_2$ was determined by comparing its absorbance with that of a $H_2O_2$ standard curve according to the manufacturer's instructions.

The fluorescence intensity of MitoSOX was measured in live cells using Laser scanning confocal microscope analysis (LSCM) Leica TCS SP8 microscope. Images were collected using a 60× objective to view cells seeded onto fibronectin-coated glass-bottom dishes. The living cells were incubated for 10 min with 2.5 μM MitoSOX probe, washed with Hanks' buffered salt solution (20 mM Hepes, pH 7.4, 135 mM NaCl, 5 mM KCl, 0.4 mM KH2PO4, 1 mM MgSO4, 0.1% w/v glucose, 1 mM CaCl2), and examined by LSCM. The red fluorescence intensity of MitoSOX was analyzed by exciting the sample with a HeNe laser 543 (excitation wavelength of 543 nm). Acquisition, storage, and data analysis were done using Leica software.

### 2.6. Western blot analysis

Total cell proteins were extracted in RIPA buffer containing protease and phosphatase inhibitor cocktails (Sigma-Aldrich Corp.) as described before [10,11]. Briefly, 60 μg of boiled proteins were loaded onto 10% sodium dodecyl sulfate-polyacrylamide electrophoresis gels, then were electro-blotted onto nitrocellulose membranes and blocked for 1 h in 5% milk. Membranes were incubated overnight at 4 °C with the primary antibody HNE (Millipore Corporation, Billerica, MA, USA) and with horseradish peroxidase-conjugated secondary antibody (BioRad, Milan, Italy). For protein involved in mitochondrial biogenesis, nitrocellulose membranes were treated with 5% (w/v) fatty acid free dry milk in 500 mM NaCl, 20 mM Tris, 0.05% Tween 20 pH 7.4 (TTBS) for 4 h at 4 °C. As specified in the legends to figures, membrane separate samples were incubated overnight at 4 °C with primary antibodies directed against PGC1α (1:1000) (Millipore), NRF1 (1:500) (Abcam), TFAM (1:500) (GeneTex), CREB (1:1000), P-CREB (Ser 133) specific against its PKA phosphorylation site (1:1000) (Santa Cruz Biotechnology), C-PKA (1:1000) (Santa Cruz Biotechnology). The level of the specific immunoblotted proteins was normalized by reprobing the blots with β-actin (Sigma) monoclonal antibodies. Proteins were detected by chemiluminescent Lite Ablot reagent (Euroclone). All images of the bands were digitized and the densitometry of the bands was performed using Quantity One-4.4.1 imaging software (Bio-Rad Laboratories).

### 2.7. Preparation of cell lysate for enzymatic assay

Confluent fibroblasts were washed, scrapped in PBS and centrifuged at 800 rcf for 10 min. Pellet was re-suspended in cold lysis buffer (50 mM Hepes, 150 mM NaCl, 1 mM $Na_3VO_4$, 100 μM NaF, 1%, 0.5 mM EDTA, 1 mM PMSF and protease inhibitor cocktail from Sigma-Aldrich). The suspension was then incubated at 4 °C for 30 min and centrifuged at 10,000 *g* for 30 min. After centrifugation, the protein concentration of the supernatant was measured by Bradford method [12].

### 2.8. NADPH oxidase (NOX) activity assay

Cell pellet was re-suspended in cold Krebs Buffer with 1 mM PMSF and protease inhibitor cocktail (Sigma-Aldrich). The cellular debris was then homogenated and centrifuged 10 min at 800 *g*. The supernatant obtained re-centrifuged at 4 °C, 1 h at 53,000 *g* with the resulting pellet (membrane fractions) resuspended in Krebs buffer. Membranes suspension (10 μg) was evaluated for NOX-enzyme activity in 200 μl of Krebs buffer with 50 μM lucigenin, 100 μM NADPH. The chemiluminescence was measured immediately and at 30 s intervals for 15 min. Although lucigenin is not specific for $O_2^-$, the NOX inhibitor VAS2870 (Sigma) was used to demonstrate that the source of the oxidant involved in lucigenin chemiluminescence was a NOX [10,13]. NOX activity was expressed as RLU/min/mg protein [14,15].

### 2.9. Superoxide dismutase (SOD) polyacrylamide activity assay

MnSOD and CuSOD activity were assayed by active gel method according to Weydert et al. [16]. The principle of this assay is based on the ability of $O_2^-$ to interact with nitroblue tetrazolium (NBT) reducing the yellow tetrazolium within the gel to a blue precipitate. Areas where SOD is active develop a clear area (achromatic bands) competing with NBT for the $O_2^-$. Cell Lysates (100 μg) were loaded and electrophoresed on a 8% Tris–HCl gel in non-denaturing running buffer and electrophoresed for 1 h at 35 mA. Gels were then rocked in nitroblue tetrazolium (NBT) dye (50 mM phosphate buffer pH 7.8 with 1 mM EDTA, 0.25 mM NBT and 0.5 mM riboflavin) for 5 min protected from light and then washed with deionized water. The gel was exposed to bright fluorescent light until achromatic bands were clearly visible. Densitometry was then performed on the achromatic bands using Pharos FX.

### 2.10. Glutathione reductase (GR) activity assay

GR activity was assayed according to the method of Smith and coworkers [17] which is based on the ability of the enzyme to reduce oxidized glutathione GSSG to the reduced form (GSH) which, in turn, can react with DTNB [5,5′-dithiobis(2-nitrobenzoic acid)]. Briefley, 10 μl of cell lysate were added to 240 μl reaction mix (100 mM potassium buffer, pH 7.4 with 0.1 mM NADPH, 3 mM DTNB and 10 mM GSSG). The increase in absorbance at 412 nm was spectrophotometrically monitored at 1-minute intervals over 10 min. GR activity was calculated using extinction coefficient 14,150 $M^{-1}$ $cm^{-1}$ and expressed as units per milligram protein.

### 2.11. Glutathione peroxidase (Gpx) activity assay

Gpx was assayed by indirect spectrophotometric assay in accordance with the method of Engel et al. [18]. This assay is based on the oxidation of GSH to GSSG coupled to the recycling of GSSG back to GSH utilizing GR and NADPH. Ten microliters of cell lysate were added to 240 μl of reaction mix (50 mM Tris–HCl, pH 8.0, with 0.5 mM EDTA, 0.2 mM NADPH, 1 U/ml GR, 1 mM GSH, 1 mM $NaN_3$ and 0.3 mM terbutilhydroperoxide). The decrease in NADPH absorbance was measured at 340 nm at 10-seconds intervals over 5 min. Gpx activity was calculated using extinction coefficient 6220 $M^{-1}$ $cm^{-1}$ and expressed as units per milligram protein.

### 2.12. Thioredoxin reductase (TrxR) activity assay

The activity of TrxR was assayed by a colorimetric method adapted from Holmgren and Bjornstedt [19] which is based on the reduction of 5,5′-dithio-bis(2-nitrobenzoate (DTNB) to 5′-thionitrobenzoic acid. In brief, 10 μl of cell lysates were added to 210 μl of reaction mix (100 mM phosphate buffer, pH 7.0 with 0.30 mM DTNB, 0.24 mM NADPH, 10 mM EDTA) 50 mM Tris–HCl, pH 8.0, with 0.5 mM EDTA, 0.2 mM NADPH, 1 U/ml GR, 1 mM GSH, 1 mM $NaN_3$ and 0.3 mM terbutilhydroperoxide). The reduction of DTNB was spectrophotometrically monitored at 412 nm at 10-s intervals over 1 min. TrxR activity was calculated using extinction coefficient 14,150 $M^{-1}$ $cm^{-1}$ and expressed as milliunits per milligram protein.

### 2.13. cAMP assay levels determination

Cell media was incubated with 1 ml of 0.1 M HCl for 10 min at 37 °C, scraped and centrifuged at 1300 rcf for 10 min at 4 °C. The supernatants were used to determine cAMP concentration using a direct immunoassay kit (Assay Designs, Ann Arbor, Michigan,USA) as described by the manufacturer. The cAMP level in the sample was normalized to the protein concentration and expressed as pmol/mg protein.

### 2.14. Bioenergetics profile

The Seahorse XF24 Extracellular Flux Analyzer (Seahorse Bioscience) was used to generate the bioenergetic profiles of primary fibroblasts by simultaneous measure of OCR (oxygen consumption rates) and ECAR (extracellular acidification rate) in real time as previously described [20]. Briefly, fibroblasts derived from skin biopsies of RTT patients and age matched healthy controls were seeded on a Seahorse XF-24 plate at a density of 60,000 cells per well and grown overnight in DMEM (10% of FCS and 1% Pen-Strep) at 37 °C in presence of $CO_2$. The density resulted in confluent cultures, in which cell growth was blocked by contact inhibition. After 24 h, cell medium was changed to unbuffered DMEM (XF Assay Medium — Seahorse Biosciences) supplemented with 5 mM glucose and 1 mM sodium pyruvate, and incubated 1 h at 37 °C in absence of $CO_2$. Medium and reagents were adjusted to pH 7.4 on the day of the assay. After four baseline measurements of OCR and ECAR levels, cells were challenged with sequential injections of mitochondrial toxins: 0.5 μM oligomycin (ATP synthase inhibitor), 1 μM FCCP (mitochondrial respiration uncoupler), 0.5 μM rotenone (complex I inhibitor), and 0.5 μM antimycin A (complex III inhibitor).

### 2.15. Mitochondrial potential determination

Mitochondrial potential was determined by Muse MitoPotential assay Kit (Millipore, Corporation, Billerica, MA, USA). Briefly, cells ($5 \times 10^5$ cells/ml) were suspended in PBS. Then, 95 μl of Muse Mitopotential working solution were added to the cells, then after 20 min at 37 °C, 5 μl of Muse 7ADD were added to the cell solution. Cells were analyzed by using a Muse Cell Analyzer.

### 2.16. Proteasome activity assay

Fibroblast pellets were re-suspended in proteasome lysis buffer (50 mM Tris, 5 mM $MgCl_2$, 10% glycerol, 500 μM EDTA pH 8.0, 1 mM DTT, 2 mM ATP) and an equal volume of glass beads (SIGMA). Cells were vortex 4 min and centrifuged 7 min 5.000 rpm at +4 °C. Supernatant were transfer in new cold tube and centrifuged for 30 min at 13.000 rpm at +4 °C. Supernatant obtained was used for proteasome assay using fluorescent-AMC peptides. Assays were carry out in 96-wells plate in a total volume of 100 μl per well. Samples were pre-incubate with or without proteasome inhibitor (50 μM MG132 from R&D) 45 min at 37 °C (50 μl per wells). Chymotrypsin-like, trypsin-like and caspase-like activity were measured in separate wells by

adding 50 μl of substrate at each well; respectively 200 μM Suc-LLVY-AMC; 200 μM Boc-LRR-AMC; 400 μM Z-LLE-AMC. Fluorescence were read for 60 min at 10 min intervals at λecc = 360; λemm = 465, gain 60. Results were expressed as RFU/min/mg protein using angular coefficient of interpolate line [21].

### 2.17. Statistical analysis

For all the variables tested, one-way analysis of variance (ANOVA) or Mann–Whitney U test was used. Statistical significance was indicated by a p-value < 0.05. Data were expressed as mean ± S.D. from triplicate determinations obtained in five separate experiments.

## 3. Results

### 3.1. Increased oxidative stress in RTT fibroblasts

As it is shown in Fig. 1, RTT fibroblasts evidenced a clear increase (2 fold) in $H_2O_2$ with respect to the control (Fig. 1A). It has been well known that lipid peroxidation and the formation of highly reactive aldehydes such as HNE can be induced through Fenton chemistry that is dependent upon iron and $H_2O_2$. Fig. 1B showed that RTT cells had a significant increase in HNE (circa 3 fold) protein adducts respect to the control fibroblasts. The increased oxidation of the fluorescent dye Mitosox Red, which has been suggested to detect mainly mitochondrial superoxide [22] is shown in RTT fibroblasts in Fig. 1C.

### 3.2. Increased NADPH oxidase (NOX) activity in RTT fibroblasts

One possible cellular source of $H_2O_2$ is the activation of one or more of the NADPH oxidase (NOX) enzymes [23]. As shown in Fig. 2A, NOX activity was significantly increased in RTT compared to control fibroblasts. Fig. 2B shows increased NOX activity correlated with translocation of the cytoplasmic subunits associated with NOX2, $p67^{phox}$ and $p47^{phox}$, to plasma membrane. Furthermore, to confirm the involvement of NOX in increased oxidant production, RTT fibroblasts were pre-treated with DPI, a general inhibitor of flavoproteins including NOX. DPI pretreatment largely prevented the formation of HNE protein adducts as shown in Fig. 2C. In addition, the pre-treatment with desferal, a well known iron chelator, decreased HNE protein adducts formation (Fig. 2D).

### 3.3. Defensive enzyme activities in RTT fibroblasts

To understand the source and the mechanisms behind the increased levels of oxidants in RTT patients, several enzymes that are involved in protecting the cells from oxidative stress were analyzed in primary skin fibroblasts. As shown in Fig. 3A, the activity levels of glutathione peroxidases (Gpx), the enzymes catalyzing the glutathione-dependent reduction of lipid hydroperoxides to their corresponding alcohol and that of $H_2O_2$ to water, were significantly lower in RTT cells than controls. The same trend was observed for glutathione reductase (Fig. 3B), the enzyme catalyzing reduction of glutathione disulfide (GSSG) to its reduced form GSH. Superoxide dismutases (SOD) catalyze the dismutation of $O_2^{\cdot-}$ to $H_2O_2$ and as it is shown in Fig. 3C, RTT cells had a significant lower activity of both mitochondrial manganese-containing SOD and cytosolic copper- and zinc-containing SOD than respective controls. Also the activity of TrxR, which participates in thiol-dependent cellular reductive processes including the reduction of $H_2O_2$, showed a significant decrease activity in RTT fibroblasts (Fig. 3D).

### 3.4. Mitochondrial bioenergetic levels in RTT fibroblasts

Fibroblasts derived from RTT patients feature overall suppressed bioenergetics as indicated by reduction of both basal and FCCP-stimulated maximal respiration (Fig. 4A), which also implies diminished mitochondrial reserve capacity. Because the latter reflects the

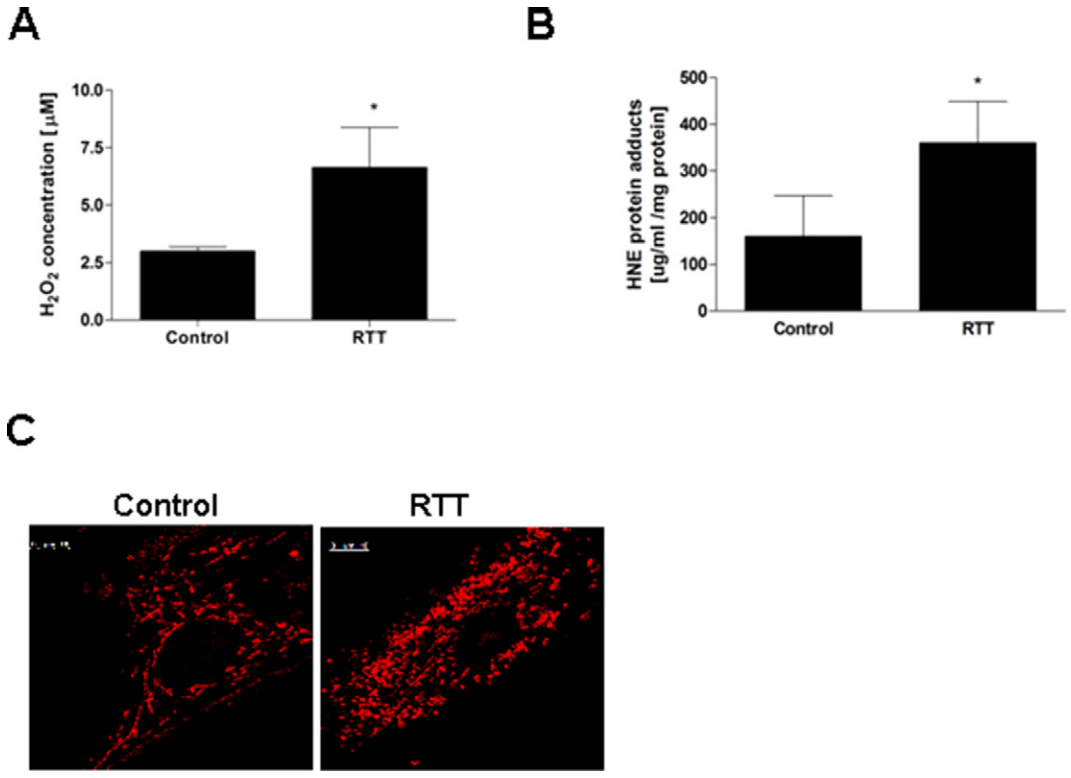


**Fig. 1.** High levels of oxidative stress are presented in RTT fibroblasts (A) RTT fibroblasts showed higher levels of $H_2O_2$ than controls measured by using Amplex red hydrogen peroxide/peroxidase assay kit. Data are expressed in μM and are the averages of five different experiments (*p < 0.05 vs control). (B) HNE protein adduct levels measured by OxiSelect HNE-His adduct ELISA kit (Cell biolabs, inc.). Data are expressed in μg/ml per mg of proteins (averages of five different experiments (*p < 0.05 vs control)). Values showed in the graph represent means ± SD. Data were analyzed by Mann–Whitney U test. (C) RTT fibroblasts presented higher MitoSOX™ Red fluorescence dye than controls.

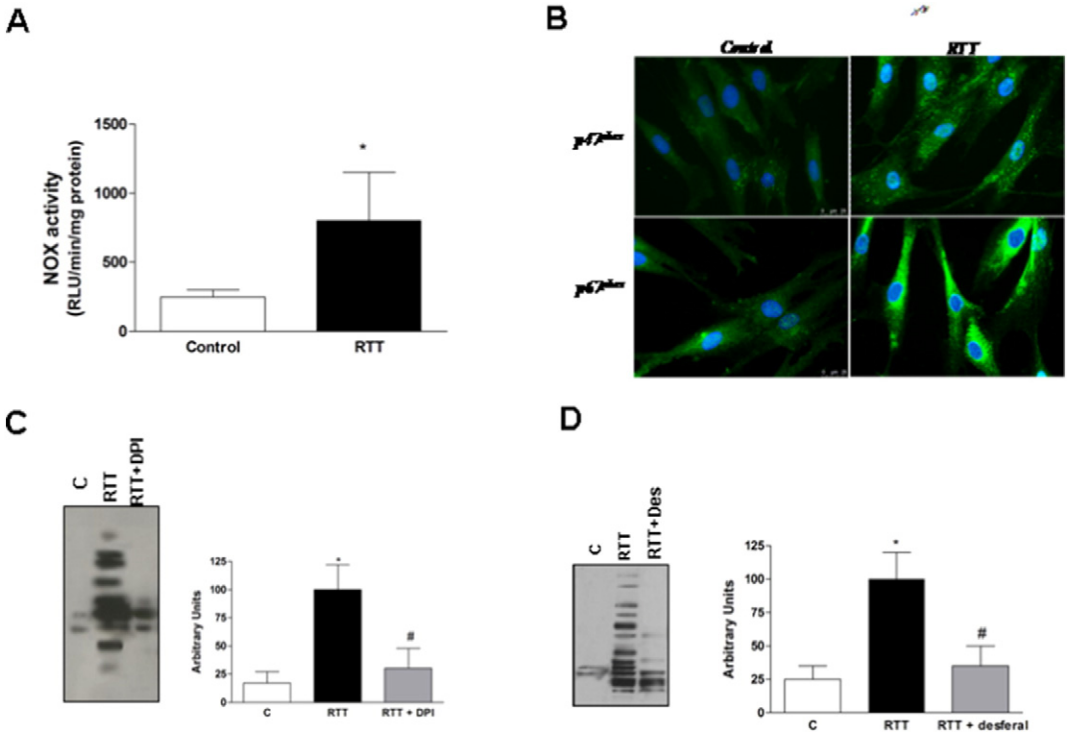


**Fig. 2.** Constitutive activation of NADPH oxidase 2 (NOX2) in RTT cells. The activity of NOX was determined by luminescent assay (A) and by immunofluorescence, by measuring the membrane translocation of p67 and p47 (B). HNE protein adduct levels were reversed by dipheyleneiodonium Chloride (DPI) (C) and desferal (Iron chelator) (D) in RTT cells. Representative Western blots of five independent experiments are shown on the left of the plot. Quantification of the HNE protein adducts bands is shown on the right panel. Data are expressed in arbitrary units (*$p < 0.05$). Data were analyzed by Mann–Whitney U test.

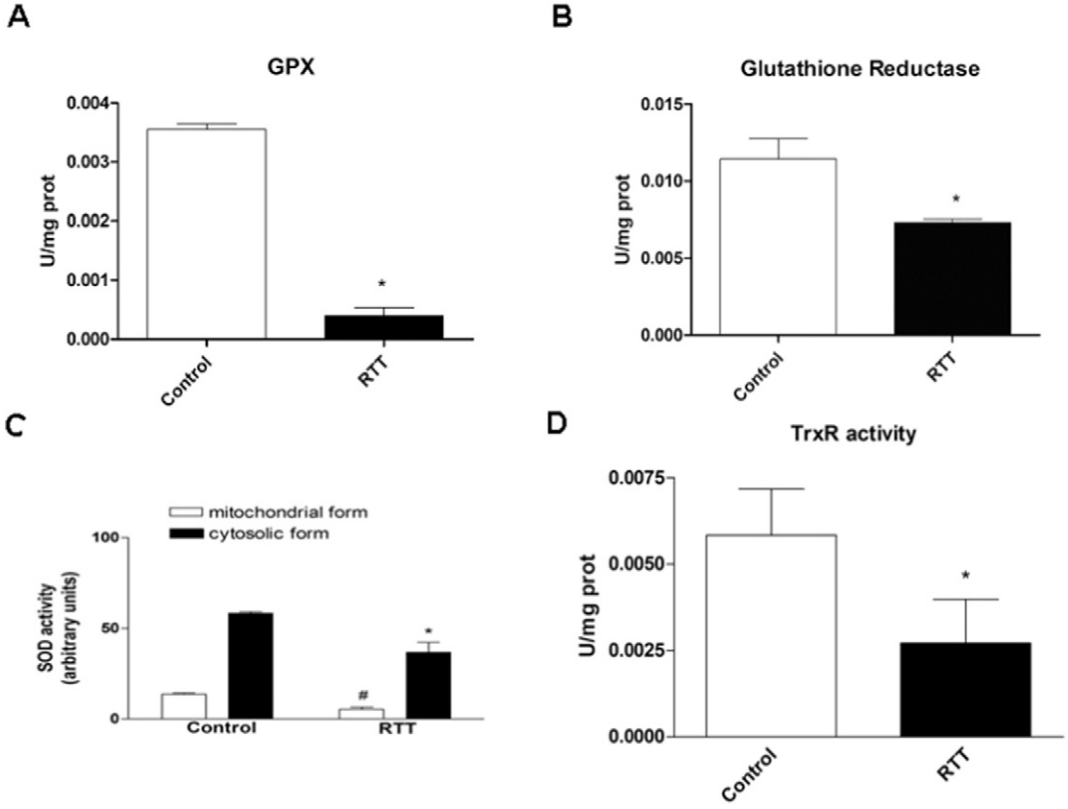


**Fig. 3.** Alteration of specific enzymes activity involved in cellular redox balance in RTT fibroblasts. (A) GPx activity, (B) GR activity, (C) Cu, Zn-SOD (cytosolic form) and Mn-SOD (mitochondrial form), (D) TrxR. Values were expressed as U/mg proteins in RTT ($n = 6$) and control ($n = 6$) fibroblasts and represent means ± SD. Data were analyzed by Mann–Whitney U test *, $p < 0.05$ vs. control. For SOD activity: *, $p < 0.05$ vs. control of cytosolic form; #, $p < 0.05$ vs control of mitochondrial form.

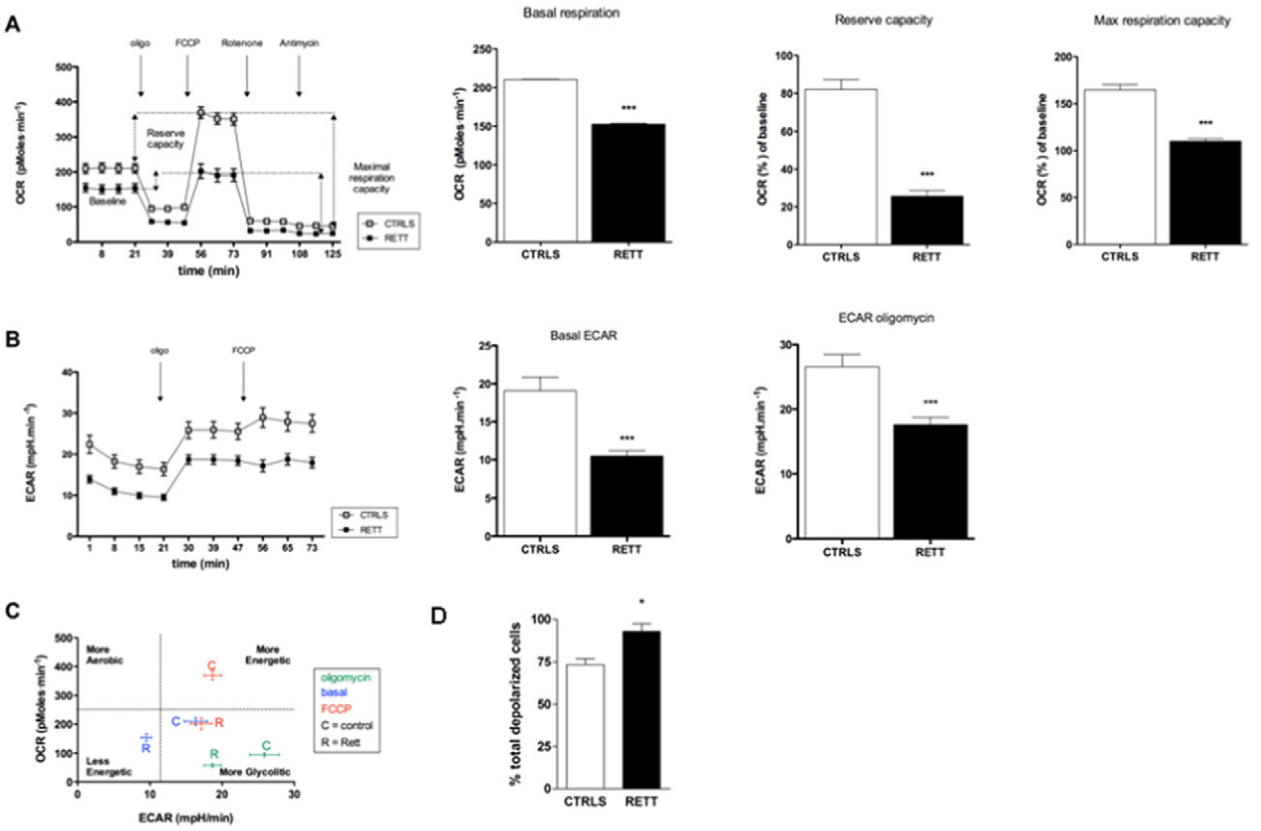


**Fig. 4.** Bioenergetic profile in RTT fibroblasts. (A) Mitochondrial function is suppressed in patients, as indicated by decreased basal and maximal respiration, as well as respiratory reserve capacity. (B) Glycolysis induced medium acidification is decreased in patients, as indicated by lower ECAR in basal and oligomycin stimulated conditions. (C) Metabolic profile based on comparison of OCR and ECAR shows that Rett fibroblasts are overall less energetic and positioned in the lower-left portion of the graph, and less responsive to stimulation with both oligomycin (for ECAR) or FCCP (for OCR). Graphs show pooled data of seven independent replicates, on three different cell lines. (D) Fibroblasts were stained with the Muse Mitopotential kit and acquired on the Muse Cell Analyzer to order to measure the total depolarized cells.

bioenergetic reservoir available to counteract cellular stress [24], our findings indicate potential vulnerability of RTT fibroblasts. Also glycolysis – which was measured as lactate dehydrogenase mediated acidification of the medium upon conversion of pyruvate – was decreased in RTT cells (Fig. 4B), both in basal conditions and upon stimulation with the mitochondrial ATP synthase inhibitor oligomycin. Overall, RTT fibroblasts feature a less energetic metabolic profile (i.e. both mitochondrial respiration and glycolysis are decreased) and exhibit a reduced

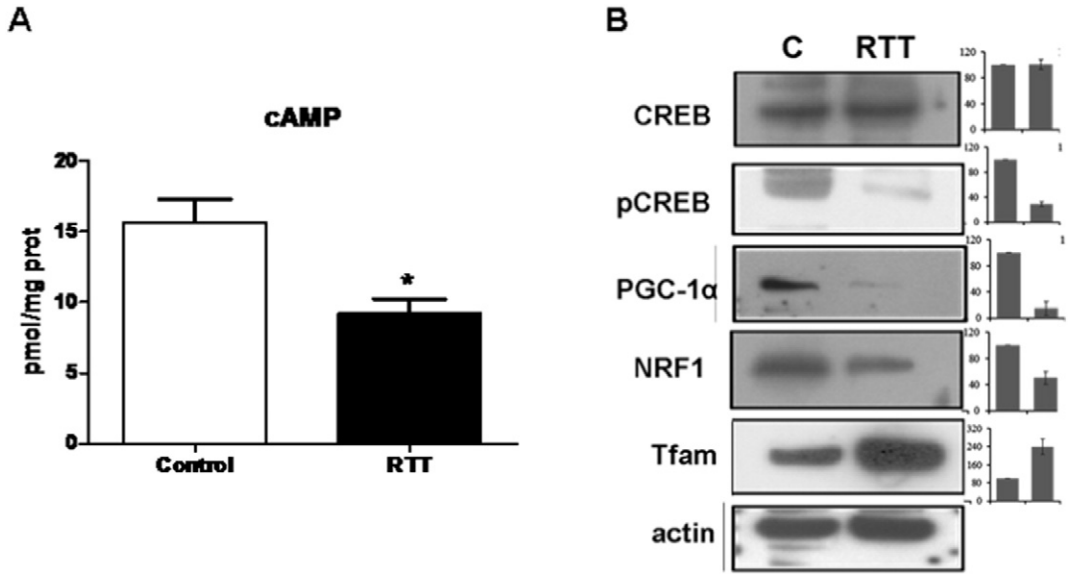


**Fig. 5.** Alteration of mitochondrial biogenesis in RTT fibroblasts. (A) RTT fibroblast levels of cAMP measured by direct immunoassay kit (Assay Designs, Ann Arbor, Michigan, USA). The cAMP level in the sample was normalized to the protein concentration and expressed as pmol/mg protein (averages of five different experiments, $^*p < 0.05$). (B) RTT fibroblasts levels of CREB, PGC-1α, NRF1 and Tfam proteins. Representative Western blot of five experiments is shown in the figure. Quantification of the protein bands is shown in the right panel. Protein loading was assessed by reprobing the blots with β-actin antibody. Data are expressed in arbitrary units (averages of five different experiments, $^*p < 0.05$).

response when respiration or glycolysis are stimulated respectively with FCCP or oligomycin (Fig. 4C). These observations are substantiated by mitochondrial potential measures, which indicate substantial depolarization in RTT patients' fibroblast, which display a 20% increase in the number of depolarized cells (Fig. 4D).

### 3.5. Transcription factors of mitochondrial biogenesis in RTT fibroblasts

It has been reported that the cAMP level is altered in the mouse model of RTT patients [25]. Several signal transduction pathways have been implicated in the control mitochondrial biogenesis, among which is the cAMP mediated signal transduction pathway, which results in phosphorylation of CREB [26,27]. In RTT fibroblasts, we found a reduced cAMP level (Fig. 5A) associated with a decrease of p-CREB with respect to the total CREB content. In agreement with the results described, PGC-1α protein expression appeared to be down-regulated as well as a protein level of PGC-1α downstream target gene, directly involved in mitochondrial biogenesis, nuclear respiratory factor 1 (NRF1). The mitochondrial transcriptor factor (Tfam), whose expression is in turn primed by NRF1 [28], was found to be up-regulated in RTT (Fig. 5B).

### 3.6. Proteasome activity in RTT fibroblasts

During oxidative stress, cells rely primarily on proteasome-mediated protein degradation for effective removal of oxidized or damaged proteins. On the other hand, modified proteins cannot be efficiently degraded because an overload of the proteasome machinery and these modified proteins can induce noxious effect in the cells. As it is shown in Fig. 6, the proteasomes of RTT fibroblasts showed a trend toward a decrease in enzymatic activity, when compared to controls. In particular, caspase- and chymotrypsin-like activities exhibited the largest decrease (−58% and −62% respectively), whereas the reduction of trypsin-like was less evident (18%).

## 4. Discussion

The principal objective of our study was to determine the possible sources and the mechanisms that are behind the increased systemic oxidative stress present in RTT patients. Our study was performed in primary skin fibroblasts isolated from RTT patients because this biological setup constitutes one of the most reliable approaches to investigate molecular and cellular mechanisms in genetic and neurological disorders [29]. Our goal here was to extend our previous study in which oxidative stress was detected in several RTT models [8,9]. As is well known, increased oxidative stress leads to lipid peroxidation and consequent production of reactive aldehydes, among which HNE is one of the most significant physiologically. In general, the biochemical effects of HNE can be explained by its high reactivity toward amino acid thiol- (cysteine) and amino-groups (histidine and lysine) that, either free or protein-bound, readily undergoes Michael addition. Therefore, HNE-mediated amino acid modifications such as those observed in oxidative stress conditions in RTT fibroblasts, may greatly alter protein activities. These alterations may subsequently produce abnormal physiological cell functions. HNE adduction contributes to the pool of damaged proteins that increases during aging and in several pathological states [30]. Furthermore, impaired protein clearance through the ubiquitin proteasome system dysfunction and/or the overwhelming production of abnormal proteins plays an important role in the pathophysiology of disorders related to oxidative stress, particularly in neuropathologies [31]. The presence of HNE has been demonstrated also in human RTT patients, and animal and ex-vivo models [8,9,32,33]. We have confirmed this in the present cell culture study. HNE adduction of brain proteins has been implicated in the etiology and/or progression of neurodegenerative disorders including Alzheimer's disease (AD), Parkinson's disease (PD), amyotrophic lateral sclerosis (ALS) and multiple sclerosis (MS) [34,35]. In addition the reduced activation of the proteasome detected in RTT cells could contribute to accumulate damaged proteins and affect cell functions.

The next question was to determine the possible source of oxidative stress present in RTT, and also whether this altered redox status could depend upon altered enzymatic activities. Therefore, we first examined the activity of endogenous sources of $O_2^{\cdot-}$ and $H_2O_2$ including the NOX proteins. Plasma membrane NOXs, including NOX1 and NOX2, serve the purpose of producing $O_2^{\cdot-}$ and $H_2O_2$ in response to stimuli through receptor-mediated signaling and therefore differ from mitochondrial $O_2^{\cdot-}$ production, which is a leak from the electron transport system [36,37] and NOX4, which is a constitutively active intracellular NOX that is regulated by its expression. Excessive amounts of oxidant production can be detrimental, resulting in the oxidative stress that appears to play an important role in numerous degenerative diseases [38,39]. In our model we found a clearly increased activation of NOX in RTT cells that is most likely due to NOX2. We conclude this because the translocation of the cytosolic subunits $p47^{phox}$ and $p67^{phox,}$ which must associate with NOX2 to activate its $O_2^{\cdot-}$ production, also occurred. This suggests that the increased oxidative stress may depend, at least in part, on NOX2 activation. The $O_2^{\cdot-}$ produced by NOX2 will rapidly dismutate to form $H_2O_2$ and $O_2$. Once produced, $H_2O_2$ can trigger lipid peroxidation through the iron-catalyzed Fenton reaction as confirmed by the elevated HNE found in the RTT fibroblasts. In our study, DPI (a general inhibitor of NOX) added at the time of cell seeding attenuated HNE protein adducts. Inhibition of HNE-adduct formation was also observed when the iron chelator (desferal) was added at the time of cell seeding, suggesting a role of NOX2-induced HNE adducts formation in RTT fibroblasts.

Oxidative stress in RTT fibroblasts could be related not only to an increased oxidant production, but also to the altered activity of enzymes mostly involved in removing $O_2^{\cdot-}$ and $H_2O_2$. We found that the activity of both forms of intracellular SOD, Cu–Zn-SOD and Mn-SOD, as well as GPx activity were lower in RTT fibroblasts compared to controls.

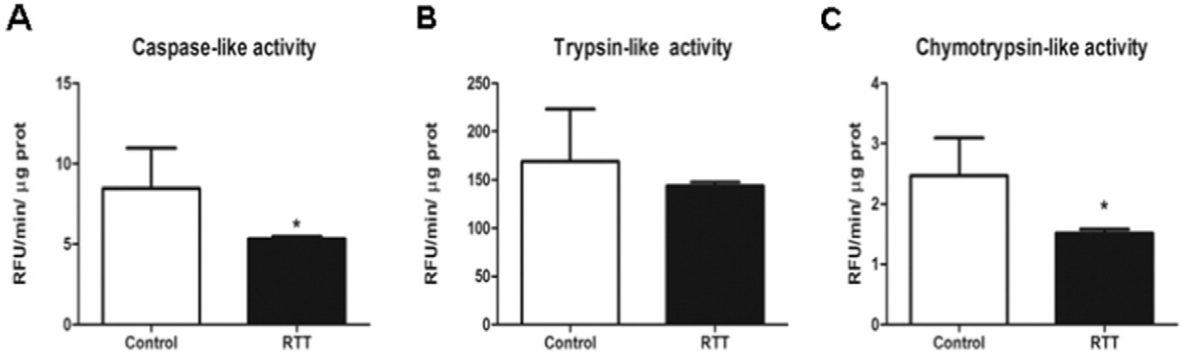


**Fig. 6.** Proteasome activities in RTT fibroblasts. (A) Chymotrypsin-like (Suc-LLVY-AMC); (B) trypsin-like (Boc-LRR-AMC), Caspase-like (Z-LLE-AMC) proteasome activities measured using fluorescent labeled proteasome substrates, in control (n = 6) and RTT (n = 6) fibroblasts. Activity was express as RFU/min/µg protein and data were analyzed by t-test *, $p < 0.05$ vs. control.

Peroxiredoxins also reduce $H_2O_2$ with five of the six isoforms in mammalian cells using either of the two isoforms of thioredoxin (Trx) [40]. Trx are proteins with critical thiols that form an intramolecular disulfide in the peroxiredoxin catalyzed reduction of $H_2O_2$, similar to the way GSSG is formed by GPxs. Oxidative stress also results in disulfides forming in proteins. Trx is used in conjunction with protein disulfide isomerase to reduce protein disulfides. The reduction of the disulfide form of Trx also depends upon NADPH via thioredoxin reductase (TrxR) activity [41]. Thus, the decreased activity of TrxR in RTT cells compared to controls adds further understanding of how oxidative stress occurs in RTT. Overall, these data confirm the relevance of mechanisms controlling thiol/disulfide equilibria in the pathogenesis RTT and, in this respect, extend to neurodevelopmental disorders previous findings obtained in chronic neurodegenerative diseases [42,43]. It should be also mentioned that in previous work we have detected a decreased levels of GSH in RTT cells [44] and this can indirectly affect TrxR by maintaining Trx in the reduced state during oxidative stress. Although GSH does not directly interact with TrxR.

The most important parameter determining the biological impact of the antioxidant enzymes is activity of the enzymes rather than their mRNA or protein. Our results have clearly show that RTT cells have lower activities of key defensive enzymes, SOD, GPx, G6PDH, and TrxR, while the pro-oxidant enzymes NOX2 activity was increased. The increased Mitosox fluorescence in RTT implied that mitochondrial $O_2^-$ production was also increased although the measurement may actually reflect the decreased Mn-SOD or other antioxidant enzymatic activities as the specificity of Mitosox is questionable [45]. Mitochondria generate $O_2^-$ from different redox centers in the respiratory chain and $H_2O_2$ from some mitochondrial enzymes as well [46]. The $O_2^-$ is rapidly dismutated by Mn-SOD or reacts with NO to form ONOO-. At low levels, it is thought that mitochondrial $H_2O_2$ plays a role in cell signaling, but, at higher rates of $H_2O_2$ production, mitochondrial proteins become susceptible to damage. Mitochondria have a relatively high concentration of both oxidizable lipids and abundant redox-active proteins that can amplify oxidative damage [46,47].

The first supportive evidence for mitochondrial defects in RTT arose from altered mitochondrial morphology. Electron microscopy of muscle and frontal lobe biopsy tissues from individual patients revealed enlarged and swollen mitochondria with electron-translucent appearance, irregular cristae, vacuolizations and granular inclusions [48]. Mitochondrial dysfunction and its derived oxidative stress may contribute to RTT pathogenesis. Indeed, some RTT clinical signs such as hypotonia [49] and myocardial dysfunctions [50] correlate with mitochondrial dysfunctions and oxidative stress. In muscle and frontal lobe biopsies of RTT patients [48,51,52] and in cortex and hippocampus of MeCP2 −/y mice [53], morphological alterations of mitochondria have been found. Furthermore a reduced NADH cytochrome c reductase, succinate cytochrome c reductase, and cytochrome c oxidase activity has been shown in muscle and frontal cortex biopsies of RTT patients [54,55] as well as an alteration of mitochondrial respiration efficiency [56]. Indeed, biochemical analyses on muscle biopsy material confirmed reduced activities of NADH cytochrome c reductase, succinate cytochrome c reductase and cytochrome c oxidase, even in mitochondria of physiological appearance [54]. These data correlate with a recent microarray analyses on RTT patient blood samples where we have noticed an up-regulation of several mitochondria-related genes [57]. Specifically, the most significantly regulated transcripts included those encoding for several subunits of mitochondrial respiratory chain complexes and thus linked directly to mitochondrial ATP production and, indirectly, to potential oxidant generation. Overall, these elements are in full agreement with our findings demonstrating altered bioenergetics profiles in RTT fibroblasts.

Our results also demonstrated the up-regulation of genes related to protein degradation and ubiquitination. This could also be a consequence of oxidized protein and the presence of HNE protein adducts. It also seems that RTT is accompanied by an increased metabolic demand and hence intensified mitochondrial activity. The cAMP pathway has been found to play also a central role in neurodevelopmental disorders and neurodegenerative diseases such as autism, Alzheimer's, Parkinson's, Huntington's disease and Down syndrome [25,27]. Recently a disturbance of the cAMP homeostasis has been proposed also in MeCP2 −/y mice [58], and moreover, it has been shown that β2-Adrenergic receptor agonist ameliorates phenotypes in a mouse model of RTT [59]. As cAMP signaling has been shown to regulate OXPHOS activity and biogenesis [28,60], we investigated cAMP-dependent mitochondrial biogenesis. The results showed that reduced cAMP in RTT were associated with reduced protein expression of transcription factors of mitochondrial biogenesis. Interestingly, Tfam appears to be up-regulated in RTT. This could be due to the reduced cAMP, as PKA-dependent phosphorylation results in the inability of Tfam protein to bind DNA and leads to Tfam degradation by Lon protease [61].

In summary, in RTT cells increased mitochondrial and NOX2 production of oxidants accompanied by decreased antioxidant defenses and impaired proteasome activity result in oxidative stress leading to damage to cell constituents and pathology.

## Authorship

1) *Carlo Cervellati*: drafting the article and substantial contributions to interpretation of data;
2) *Claudia Sticozzi*: drafting the article, substantial contributions to conception and design, acquisition of data, analysis and interpretation of data;
3) *Arianna Romani*: substantial contributions to acquisition of data, analysis and interpretation of data;
4) *Giuseppe Belmonte*: substantial contributions to acquisition of data, analysis of data;
5) *Domenico De Rasmo*: substantial contributions to acquisition of data, analysis and interpretation of data;
6) *Anna Signorile*: substantial contributions to acquisition of data, analysis and interpretation of data;
7) *Franco Cervellati*: substantial contributions to acquisition of data, analysis and interpretation of data;
8) *Chiara Milanese*: substantial contributions to acquisition of data, analysis and interpretation of data;
9) *Pier Giorgio Mastroberardino*: substantial contributions to acquisition of data, analysis and interpretation of data; revising it critically for important intellectual content;
10) *Alessandra Pecorelli*: revising it critically for important intellectual content;
11) *Vinno Savelli*: revising it critically for important intellectual content;
12) *Henry J Forman*: revising it critically for important intellectual content and substantial contributions to interpretation of data;
13) *Joussef Hayek*: revising it critically for important intellectual content;
15) *Giuseppe Valacchi*: revising it critically for important intellectual content and substantial contributions to interpretation of data, supervising the work and final approval of the version to be published.

## Acknowledgments

AIRETT and UNICOOP Firenze for partial support and Mr. Andrea Margutti for technical support.

## References

[1] B. Hagberg, Clinical manifestations and stages of Rett syndrome, Ment. Retard. Dev. Disabil. Res. Rev. 8 (2) (2002) 61–65.
[2] J. Guy, H. Cheval, J. Selfridge, A. Bird, The role of MeCP2 in the brain, Annu. Rev. Cell Dev. Biol. 27 (2011) 631–652.
[3] D.T. Lioy, S.K. Garg, C.E. Monaghan, J. Raber, K.D. Foust, B.K. Kaspar, P.G. Hirrlinger, F. Kirchhoff, J.M. Bissonnette, N. Ballas, G. Mandel, A role for glia in the progression of Rett's syndrome, Nature 475 (7357) (2011) 497–500.
[4] J. Guy, J. Gan, J. Selfridge, S. Cobb, A. Bird, Reversal of neurological defects in a mouse model of Rett syndrome, Science 315 (5815) (2007) 1143–1147.

[5] C. De Felice, C. Signorini, T. Durand, C. Oger, A. Guy, V. Bultel-Poncé, J.M. Galano, L. Ciccoli, S. Leoncini, M. D'Esposito, S. Filosa, A. Pecorelli, G. Valacchi, J. Hayek, F2-dihomo-isoprostanes as potential early biomarkers of lipid oxidative damage in Rett syndrome, J. Lipid Res. 52 (12) (2011) 2287–2297.

[6] S. Leoncini, C. De Felice, C. Signorini, A. Pecorelli, T. Durand, G. Valacchi, L. Ciccoli, J. Hayek, Oxidative stress in Rett syndrome: natural history, genotype, and variants, Redox Rep. 16 (4) (2011) 145–153.

[7] C. Signorini, C. De Felice, S. Leoncini, A. Giardini, M. D'Esposito, S. Filosa, F. Della Ragione, M. Rossi, A. Pecorelli, G. Valacchi, L. Ciccoli, J. Hayek, $F_4$-neuroprostanes mediate neurological severity in Rett syndrome, Clin. Chim. Acta 412 (15-16) (2011) 1399–1406.

[8] A. Pecorelli, L. Ciccoli, C. Signorini, S. Leoncini, A. Giardini, M. D'Esposito, S. Filosa, J. Hayek, C. De Felice, G. Valacchi, Increased levels of 4HNE-protein plasma adducts in Rett syndrome, Clin. Biochem. 44 (5-6) (2011) 368–371.

[9] C. De Felice, F. Della Ragione, C. Signorini, S. Leoncini, A. Pecorelli, L. Ciccoli, F. Scalabrì, F. Marracino, M. Madonna, G. Belmonte, L. Ricceri, B. De Filippis, G. Laviola, G. Valacchi, T. Durand, J.M. Galano, C. Oger, A. Guy, V. Bultel-Poncé, J. Guy, S. Filosa, J10. Hayek, M. D'Esposito, Oxidative brain damage in Mecp2-mutant murine models of Rett syndrome, Neurobiol. Dis. 68 (2014) 66–77.

[10] C. Sticozzi, G. Belmonte, A. Pecorelli, B. Arezzini, C. Gardi, E. Maioli, C. Miracco, M. Toscano, H.J. Forman, G. Valacchi, Cigarette smoke affects keratinocytes SRB1 expression and localization via H2O2 production and HNE protein adducts formation, PLoS One 7 (3) (2012) e33592.

[11] G. Valacchi, P.A. Davis, E.M. Khan, R. Lanir, E. Maioli, A. Pecorelli, C.E. Cross, T. Goldkorn, Cigarette smoke exposure causes changes in scavenger receptor B1 level and distribution in lung cells, Int. J. Biochem. Cell Biol. 43 (7) (2011) 1065–1070.

[12] M.M. Bradford, A rapid and sensitive method for the quantitation of microgram quantities of protein utilizing the principle of protein-dye binding, Anal. Biochem. 72 (1–2) (1976) 248–254.

[13] M.R. Yun, H.M. Park, K.W. Seo, S.J. Lee, D.S. Im, C.D. Kim, 5-Lipoxygenase plays an essential role in 4-HNE-enhanced ROS production in murine macrophages via activation of NADPH oxidase, Free Radic. Res. 44 (7) (2010) 742–750.

[14] N.D. Magnani, T. Marchini, V. Vanasco, D.R. Tasat, S. Alvarez, P. Evelson, Reactive oxygen species produced by NADPH oxidase and mitochondrial dysfunction in lung after an acute exposure to residual oil fly ashes, Toxicol. Appl. Pharmacol. 270 (1) (2013) 31–38.

[15] N. Kartner, N. Alon, M. Swift, M. Buchwald, Riordan wr JR. Isolation of plasma membranes from human skin fibroblasts, J. Membr. Biol. 36 (1) (1977) 191–211.

[16] C.J. Weydert, J.J. Cullen, Measurement of superoxide dismutase, catalase and glutathione peroxidase in cultured cells and tissue, Nat. Protoc. 5 (1) (2010) 51–66.

[17] I.K. Smith, T.L. Vierheller, C.A. Thorne, Assay of glutathione reductase in crude tissue homogenates using 5,5′-dithiobis(2-nitrobenzoic acid), Anal. Biochem. 175 (2) (1988) 408–413.

[18] H.J. Engel, W. Domschke, M. Alberti, G.F. Domagk, Protein structure and enzymatic activity. II. Purification and properties of a crystalline glucose-6-phosphate dehydrogenase from Candida utilis, Biochim. Biophys. Acta 191 (1969) 509–516.

[19] A. Holmgren, M. Björnstedt, Thioredoxin and thioredoxin reductase, Methods Enzymol. 252 (1995) 199.

[20] G. Ambrosi, C. Ghezzi, S. Sepe, C. Milanese, C. Payan-Gomez, C.R. Bombardieri, M.T. Armentero, R. Zangaglia, C. Pacchetti, P.G. Mastroberardino, F. Blandini, Bioenergetic and proteolytic defects in fibroblasts from patients with sporadic Parkinson's disease, Biochim. Biophys. Acta 1842 (9) (2014) 1385–1394.

[21] Z. Cui, S.M. Hwang, A.V. Gomes, Identification of the immunoproteasome as a novel regulator of skeletal muscle differentiation, Mol. Cell. Biol. 34 (1) (2014) 96–109.

[22] P. Mukhopadhyay, M. Rajesh, K. Yoshihiro, G. Haskó, P. Pacher, Simple quantitative detection of mitochondrial superoxide production in live cells, Biochem. Biophys. Res. Commun. 358 (1) (2007) 203–208.

[23] G. Cheng, Z. Cao, X. Xu, E.G. van Meir, J.D. Lambeth, Homologs of gp91phox: cloning and tissue expression of Nox3, Nox4, and Nox5, Gene 269 (1–2) (2001) 131–140.

[24] B.G. Hill, B.P. Dranka, L. Zou, J.C. Chatham, V.M. Darley-Usmar, Importance of the bioenergetic reserve capacity in response to cardiomyocyte stress induced by 4-hydroxynonenal, Biochem. J. 424 (1) (2009) 99–107.

[25] S.L. Mironov, E.Y. Skorova, S. Kügle, r Epac-mediated cAMP-signalling in the mouse model of Rett Syndrome, Neuropharmacology 60 (2011) 869–877.

[26] J. Lin, C. Handschin, B.M. Spiegelman, Metabolic control through the PGC-1 family of transcription coactivators, Cell Metab. 1 (2005) 361–370.

[27] S. Papa, D. De Rasmo, Complex I deficiencies in neurological disorders, Trends Mol. Med. 19 (1) (2013) 61–69.

[28] D. De Rasmo, A. Signorile, F. Papa, E. Roca, S. Papa, cAMP/Ca2 + response element-binding protein plays a central role in the biogenesis of respiratory chain proteins in mammalian cells, IUBMB Life 62 (6) (2010) 447–452.

[29] G. Auburger, M. Klinkenberg, J. Drost, K. Marcus, B. Morales-Gordo, W.S. Kunz, U. Brandt, V. Broccoli, H. Reichmann, S. Gispert, M. Jendrach, Primary skin fibroblasts as a model of Parkinson's disease, Mol. Neurobiol. 46 (1) (2012) 20–27.

[30] K. Uchida, 4-Hydroxy-2-nonenal: a product and mediator of oxidative stress, Prog. Lipid Res. 42 (4) (2003) 318–343.

[31] T. Grune, K.J. Davies, The proteasomal system and HNE-modified proteins, Mol. Asp. Med. 24 (4-5) (2003) 195–204.

[32] L. Ciccoli, C. De Felice, E. Paccagnini, S. Leoncini, A. Pecorelli, C. Signorini, G. Belmonte, R. Guerranti, A. Cortelazzo, M. Gentile, G. Zollo, T. Durand, G. Valacchi, M. Rossi, J. Hayek, Erythrocyte shape abnormalities, membrane oxidative damage, and β-actin alterations: an unrecognized triad in classical autism, Mediat. Inflamm. 2013 (2013) 432616.

[33] C. Sticozzi, G. Belmonte, A. Pecorelli, F. Cervellati, S. Leoncini, C. Signorini, L. Ciccoli, C. De Felice, J. Hayek, G. Valacchi, Scavenger receptor B1 post-translational modifications in Rett syndrome, FEBS Lett. 587 (14) (2013) 2199–2204.

[34] L.M. Sayre, P.I. Moreira, M.A. Smith, G. Perry, Metal ions and oxidative protein modification in neurological disease, Ann. Ist. Super. Sanita. 41 (2) (2005) 143–164.

[35] J. van Horssen, G. Schreibelt, J. Drexhage, T. Hazes, C.D. Dijkstra, P. van der Valk, H.E. de Vries, Severe oxidative damage in multiple sclerosis lesions coincides with enhanced antioxidant enzyme expression, Free Radic. Biol. Med. 45 (12) (2008) 1729–1737.

[36] J.D. Lambeth, NOX enzymes and the biology of reactive oxygen, Nat. Rev. Immunol. 4 (2004) 181–189.

[37] M. Valko, D. Leibfritz, J. Moncol, M.T. Cronin, M. Mazur, J. Telser, Free radicals and antioxidants in normal physiological functions and human disease, Int. J. Biochem. Cell Biol. 39 (2007) 44–84.

[38] Z.Z. Chong, F. Li, K. Maiese, Oxidative stress in the brain: novel cellular targets that govern survival during neurodegenerative disease, Prog. Neurobiol. 75 (2005) 207–246.

[39] A. Nunomura, G. Perry, G. Aliev, K. Hirai, A. Takeda, E.K. Balraj, P.K. Jones, H. Ghanbari, T. Wataya, S. Shimohama, S. Chiba, C.S. Atwood, R.B. Petersen, M.A. Smith, Oxidative damage is the earliest event in Alzheimer disease, J. Neuropathol. Exp. Neurol. 60 (8) (2001) 759–767.

[40] S.W. Kang, H.Z. Chae, M.S. Seo, K. Kim, I.C. Baines, S.G. Rhee, Mammalian peroxiredoxin isoforms can reduce hydrogen peroxide generated in response to growth factors and tumor necrosis factor-alpha, J. Biol. Chem. 273 (1998) 6297–6302.

[41] E.S. Arnér, A. Holmgren, Physiological functions of thioredoxin and thioredoxin reductase, Eur. J. Biochem. 267 (20) (2000) 6102–6109.

[42] P.G. Mastroberardino, A.L. Orr, X. Hu, H.M. Na, J.T. Greenamyre, A FRET-based method to study protein thiol oxidation in histological preparations, Free Radic. Biol. Med. 45 (7) (2008) 971–981.

[43] M.P. Horowitz, C. Milanese, R. Di Maio, X. Hu, L.M. Montero, L.H. Sanders, V. Tapias, S. Sepe, W.A. van Cappellen, E.A. Burton, J.T. Greenamyre, P.G. Mastroberardino, Single-cell redox imaging demonstrates a distinctive response of dopaminergic neurons to oxidative insults, ARS 15 (4) (2011) 855–871.

[44] C. Signorini, S. Leoncini, C. De Felice, A. Pecorelli, I. Meloni, F. Ariani, F. Mari, S. Amabile, E. Paccagnini, M. Gentile, G. Belmonte, G. Zollo, G. Valacchi, T. Durand, J.M. Galano, L. Ciccoli, A. Renieri, J. Hayek, Redox imbalance and morphological changes in skin fibroblasts in typical Rett syndrome, Oxidative Med. Cell. Longev. 2014 (2014) 195935.

[45] B. Kalyanaraman, V. Darley-Usmar, K.J. Davies, P.A. Dennery, H.J. Forman, M.B. Grisham, G.E. Mann, K. Moore, L.J. Roberts II, H. Ischiropoulos, Measuring reactive oxygen and nitrogen species with fluorescent probes: challenges and limitations, Free Radic. Biol. Med. 52 (1) (2012) 1–6.

[46] M.P. Murphy, Mitochondria—a neglected drug target, Curr. Opin. Investig. Drugs 10 (10) (2009) 1022–1024.

[47] S.W. Ballinger, C. Patterson, C.N. Yan, R. Doan, D.L. Burow, C.G. Young, F.M. Yakes, B. Van Houten, C.A. Ballinger, B.A. Freeman, M.S. Runge, Hydrogen peroxide- and peroxynitrite-induced mitochondrial DNA damage and dysfunction in vascular endothelial and smooth muscle cells, Circ. Res. 86 (9) (2000) 960–966.

[48] M.T. Dotti, L. Manneschi, A. Malandrini, N. De Stefano, F. Caznerale, A. Federico, Mitochondrial dysfunction in Rett syndrome. An ultrastructural and biochemical study, Brain Dev. 15 (1993) 103–106.

[49] H.A. Heilstedt, M.D. Shahbazian, B. Lee, Infantile hypotonia as a presentation of Rett syndrome, Am. J. Med. Genet. 111 (2002) 238–242.

[50] C. De Felice, S. Maffei, C. Signorini, S. Leoncini, S. Lunghetti, G. Valacchi, M. D'Esposito, S. Filosa, F. Della Ragione, G. Butera, R. Favilli, L. Ciccoli, J. Hayek, Subclinical myocardial dysfunction in Rett syndrome, Eur. Heart J. Cardiovasc. Imaging 13 (2012) 339–345.

[51] M.E. Cornford, M. Philippart, B. Jacobs, A.B. Scheibel, H.V. Vinters, Neuropathology of Rett syndrome: case report with neuronal and mitochondrial abnormalities in the brain, J. Child Neurol. 9 (1994) 424–431.

[52] O. Eeg-Olofsson, A.G. al-Zuhair, A.S. Teebi, A.S. Daoud, M. Zaki, M.S. Besisso, M.M. Al-Essa, Rett syndrome: a mitochondrial disease? J. Child Neurol. 5 (1990) 210–214.

[53] P.V. Belichenko, E.E. Wright, N.P. Belichenko, E. Masliah, H.H. Li, W.C. Mobley, U. Francke, Widespread changes in dendritic and axonal morphology in Mecp2-mutant mouse models of Rett syndrome: evidence for disruption of neuronal networks, J. Comp. Neurol. 514 (2009) 240–258.

[54] S.B. Coker, A.R. Melnyk, Rett syndrome and mitochondrial enzyme deficiencies, J. Child Neurol. 6 (1991) 164–166.

[55] J.H. Gibson, B. Slobedman, K.N. Harikrishnan, S.L. Williamson, D. Minchenko, A. El-Osta, J.L. Stern, J. Christodoulou, Downstream targets of methyl CpG binding protein 2 and their abnormal expression in the frontal cortex of the human Rett syndrome brain, BMC Neurosci. 11 (2010) 53.

[56] V. Saywell, A. Viola, S. Confort-Gouny, Y. Le Fur, L. Villard, P.J. Cozzone, Brain magnetic resonance study of Mecp2 deletion effects on anatomy and metabolism, Biochem. Biophys. Res. Commun. 340 (2006) 776–783.

[57] A. Pecorelli, F. Natrella, G. Belmonte, C. Miracco, F. Cervellati, L. Ciccoli, A. Mariottini, R. Rocchi, G. Vatti, A. Bua, R. Canitano, J. Hayek, H.J. Forman, G. Valacchi, NADPH oxidase activation and 4-hydroxy-2-nonenal/aquaporin-4 adducts as possible new players in oxidative neuronal damage presents in drug-resistant epilepsy, Biochim. Biophys. Acta 1852 (3) (2015) 507–519.

[58] D. Valenti, L. de Bari, B. De Filippis, A. Henrion-Caude, R.A. Vacca, Mitochondrial dysfunction as a central actor in intellectual disability-related diseases: an overview of down syndrome, autism, fragile X and Rett syndrome, Neurosci. Biobehav. Rev. 46 (Pt 2) (2014) 202–217.

[59] N. Mellios, J. Woodson, R.I. Garcia, B. Crawford, J. Sharma, S.D. Sheridan, S.J. Haggarty, M. Sur, β2-Adrenergic receptor agonist ameliorates phenotypes and corrects microRNA-mediated IGF1 deficits in a mouse model of Rett syndrome, PNAS 111 (27) (2014) 9947–9952.

[60] D. De Rasmo, A. Signorile, M. Larizza, C. Pacelli, T. Cocco, S. Papa, Activation of the cAMP cascade in human fibroblast cultures rescues the activity of oxidatively damaged complex I, Free Radic. Biol. Med. 52 (2012) 757–764.

[61] B. Lu, J. Lee, X. Nie, M. Li, Y.I. Morozov, S. Venkatesh, D.F. Bogenhagen, D. Temiakov, C.K. Suzuki, Phosphorylation of human TFAM in mitochondria impairs DNA binding and promotes degradation by the AAA + Lon protease, Mol. Cell 49 (1) (2013) 121–132.